Human Molecular Genetics, 2011, Vol. 20, No. 1 **64–79**
doi:10.1093/hmg/ddq432
Advance Access published on October 8, 2010

Premutation CGG-repeat expansion of the *Fmr1* gene impairs mouse neocortical development

Christopher L. Cunningham[1], Verónica Martínez Cerdeño[2], Eliecer Navarro Porras[8], Anish N. Prakash[3], James M. Angelastro[5], Rob Willemsen[9], Paul J. Hagerman[3,4], Isaac N. Pessah[3,5], Robert F. Berman[3,6] and Stephen C. Noctor[3,7,*]

[1]Neuroscience Graduate Program, [2]Department of Pathology, Institute for Pediatric Regenerative Medicine–Shriners Hospital, School of Medicine, [3]Medical Investigations of Neurodevelopmental Disorders (M.I.N.D.) Institute, [4]Department of Biochemistry and Molecular Medicine, School of Medicine, [5]Department of Molecular Biosciences, School of Veterinary Medicine, [6]Department of Neurological Surgery, School of Medicine and [7]Department of Psychiatry, School of Medicine, UC Davis, Sacramento, CA, USA, [8]Brigham Young University–Idaho, Rexburg, ID, USA and [9]CBG–Department of Clinical Genetics, Erasmus MC, Rotterdam, The Netherlands

Received May 28, 2010; Revised August 20, 2010; Accepted October 1, 2010

Fragile X-associated tremor/ataxia syndrome (FXTAS) is a late adult-onset neurodegenerative disorder caused by a premutation CGG-trinucleotide repeat expansion (55–200 CGG repeats) within the 5′-untranslated region of the *FMR1* gene. Although FXTAS generally affects premutation carriers over 50 years of age, cognitive and psychological symptoms can appear in carriers during childhood, suggesting that the *FMR1* premutation affects brain function early in life. Recent work with cultured hippocampal neurons from a premutation (*Fmr1* CGG knock-in) mouse model revealed impaired development of early postnatal neurons, consistent with the developmental clinical involvement of premutation carriers. In the current work, we show that the presence of premutation CGG-repeat expansions in the mouse *Fmr1* gene alters embryonic neocortical development. Specifically, embryonic premutation mice display migration defects in the neocortex and altered expression of neuronal lineage markers. The current data demonstrate that premutation alleles of the *Fmr1* gene are associated with defects in developmental programs operating during prenatal stages of brain formation and provide further evidence that the *FMR1* premutation has a neurodevelopmental component.

INTRODUCTION

Fragile X-associated tremor/ataxia syndrome (FXTAS) is a late-onset, neurodegenerative disorder that affects carriers of premutation CGG-repeat alleles (55–200 repeats) of the fragile X mental retardation 1 (*FMR1*) gene. Core features of the disorder include progressive gait ataxia and intention tremor with associated cognitive decline and executive dysfunction, peripheral neuropathy, dysautonomia and Parkinsonism (1–7). Larger CGG-repeat expansions (full mutation; >200 CGG repeats) give rise to fragile X syndrome, the most common inherited form of cognitive impairment (8–11). Moreover, premutation alleles of the *FMR1* gene are quite common in the general population, with as many as 1:250 males and 1:130 females carrying premutation alleles (12–14). However, only a subset of carriers will develop FXTAS (15), with both clinical and neuropathological features being a function of the number of CGG repeats (16–19).

The apparent absence of FXTAS cases in the full mutation CGG-repeat range, where the *FMR1* gene is transcriptionally silent (absence of *FMR1* and mRNA protein), coupled with marked elevation of *FMR1* mRNA in the premutation range (20–22), has led to the proposal that FXTAS is caused by a toxic gain-of-function effect of the *FMR1* mRNA (23). Consistent with this hypothesis, characteristic intranuclear inclusions found in neuronal and glial cells of FXTAS cases (16,24) have been found to contain *FMR1* mRNA (25).

*To whom correspondence should be addressed at: UC Davis M.I.N.D. Institute, 2805 50th Street, Sacramento, CA 95817. Tel: +1 9167030435; Fax: +1 9167030367; Email: scnoctor@ucdavis.edu

Furthermore, formation of the intranuclear inclusions in cell culture requires only active expression of the CGG-repeat region as RNA (26), and expression of CGG repeats in Purkinje neurons produces intranuclear inclusions, neurodegeneration and motor deficits (27).

To facilitate detailed studies of brain functioning in *FMR1* premutation, a mouse model has been developed by replacing the native 9–10 CGG repeats in the mouse *Fmr1* gene with approximately 100 CGG repeats (28) (hereafter premutation mouse). The premutation mouse model shares many key features observed in human premutation carriers, both with and without FXTAS. Both adult premutation mice and adult premutation humans exhibit upregulated *FMR1*/*Fmr1* mRNA, normal to slightly decreased levels of fragile X mental retardation protein (FMRP), intranuclear inclusions in neurons and glia and neurodegeneration (28–32). Chen *et al.* (32) recently demonstrated that hippocampal neurons that were obtained from premutation mice shortly after birth and grown in culture display early functional and morphological impairments that precede neurodegeneration (32), providing further evidence that the *FMR1* premutation impacts CNS functioning during early stages of development. In this regard, *FMR1* mRNA has been reported in the human embryonic neocortex (33), and FMRP protein has been shown in the human (34) and mouse embryonic neocortex (35). These data suggest that *FMR1* gene expression could impact normal and pathogenic developmental processes in the typically developing and premutation embryonic brain.

We used *in utero* retroviral cell labeling and immunostaining methods in premutation mice and wild-type littermate controls to assess whether *Fmr1* premutation impacts the regulation of developmental processes in the embryonic neocortex. We show here that (i) precursor cells and immature neurons express FMRP in the wild-type embryonic neocortex, (ii) that neocortical neurons exhibit a migration defect in embryonic premutation mice and (iii) that there is a significant increase in the number of cells that express the precursor cell marker Pax6 and a significant decrease in the number of cells that express the neural precursor cell marker Tbr2 in premutation mice. These data are consistent with the hypothesis that premutation CGG expansions of the *Fmr1* gene impact migration and differentiation in the embryonic brain and reinforce the concept that the *FMR1* premutation impacts brain development earlier than previously described. Therefore, the defects in neocortical development that we observe in premutation mice may provide the basis for the clinical observations that children who carry the *FMR1* premutation exhibit psychological symptoms, attention deficit hyperactivity disorder (ADHD) and autism spectrum disorders (3,36,37).

RESULTS

FMRP is expressed in the embryonic neocortex

To examine FMRP expression in the embryonic brain, coronal sections of the neocortex obtained from wild-type littermates of premutation mice at embryonic day (E) 16 were immunostained with anti-FMRP antibodies. Two anti-FMRP antibodies were utilized: a commercially available mouse monoclonal antibody (clone 1C3, Millipore) and a chicken polyclonal antibody (38). The commercial antibody produced a stronger overall pattern of immunoreactivity (IR) in the embryonic brain, but this may be due in part to cross-reactivity with related FXR proteins that are also expressed in the embryonic brain (35). The chicken polyclonal antibody produced a more restricted pattern of IR in the embryonic and postnatal brain and was used for our analysis with both enzymatic and fluorescent secondary antibody staining. Strong FMRP-IR was noted in the cortical plate (CP) and subplate in dorsolateral regions of the E16 neocortex (Fig. 1A). The upper intermediate zone was relatively free from labeling. FMRP-IR was also present in the ventricular zone (VZ) and subventricular zone (SVZ) and there was a particularly strong band of FMRP-IR near the edge of the ventricle in the dorsolateral cortex (Fig. 1A, open arrowheads). The regional patterns of FMRP-IR in the embryonic cerebral cortex did not vary between wild-type and premutation mice. Positive controls produced staining patterns that matched previous descriptions of FMRP-IR in the postnatal brain (39), whereas negative controls, including *Fmr1*-KO embryonic neocortex (Fig. 1B), preimmune serum (Fig. 1D) and absence of primary antibody (data not shown), lacked IR. FMRP-IR at the edge of the ventricular lumen of embryonic rodent neocortex has been shown in previous studies (35), and the presence of *FMR1* mRNAs in the VZ, SVZ and CP has been reported in the fetal human neocortex (33). Our results confirm these findings.

To determine which cell types expressed FMRP in the embryonic neocortex, cortical tissue was double-immunostained with antibodies against FMRP and antibodies that label neural precursor cells or immature neurons. To test whether precursor cells expressed FMRP, sections of wild-type embryonic neocortex were double-labeled with antibodies directed against FMRP and antibodies that detect the phosphorylated form of vimentin (4A4). Phosphorylated vimentin is present in embryonic precursor cells only during M-phase of division (40,41) and is expressed by all radial glial cells undergoing division in the embryonic VZ and by intermediate progenitor cells undergoing division in the SVZ (41,42). FMRP expression was observed in the VZ along the edge of the ventricular lumen where radial glial precursor cells divide (Fig. 1C; white asterisks). FMRP is primarily a cytoplasmic protein (39,43), and expression was observed in the very thin rim of cytoplasm that surrounds the densely packed nuclei of dividing radial glial cells in the VZ (Fig. 1E–I). FMRP expression was also noted in the proximal portion of the pial fiber of radial glial cells (Fig. 1E and F; white arrowheads). 4A4-IR is reduced at the end of cytokinesis and ceases altogether as cells transition from M-phase into G1/G0-phase (44). FMRP expression in radial glial cells appeared stronger in those cells that were passing from M-phase to G1/G0-phase (Fig. 1I). In addition, FMRP expression was observed in mitotic cells undergoing division away from the surface of the ventricle in the SVZ (Fig. 1J). In particular, cytoplasmic FMRP expression was noted in neural precursor cells in the SVZ that expressed the nuclear transcription factor Tbr2 (Fig. 1K). FMRP was also strongly expressed by cells expressing the immature neuronal marker Tuj1 in the embryonic proliferative zones (Fig. 2). These data demonstrate that immature neurons and precursor cells express FMRP during embryonic stages of brain formation. Furthermore, these data suggest that FMRP is expressed in the embryonic neocortex in a regional and cell-specific

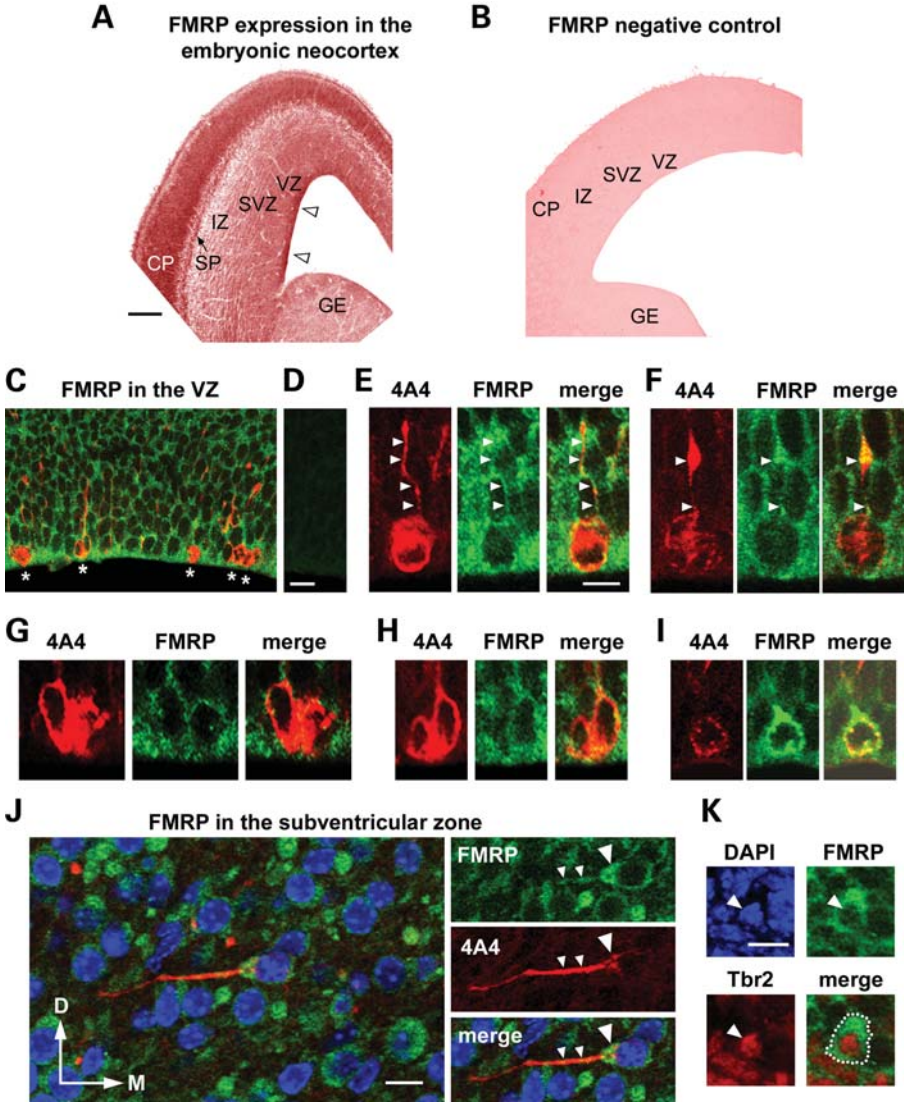

Figure 1. FMRP expression in the embryonic neocortex. (**A**) Enzymatic anti-FMRP immunostaining shows strong FMRP immunoreactivity (IR) in the cortical plate (CP), subplate (SP, black arrow), ventricular zone (VZ) and subventricular zone (SVZ). A strong band of FMRP-IR is present at the edge of the lateral ventricle in the dorsolateral neocortex (open arrowheads). (**B**) *Fmr1* KO mouse neocortex lacks FMRP-IR. (**C**) Double immunostaining with antibodies against FMRP (green) and phosphorylated vimentin (4A4, red). 4A4 labels mitotic radial glial precursor cells that divide at the edge of the lateral ventricle (white asterisks). The 4A4+ RG cells have pial fibers that course radially away from the ventricle toward the pial surface. (**D**) Negative control immunofluorescent staining of embryonic neocortex with preimmune antibodies. (**E** and **F**) FMRP-IR (green) is present in the pial fiber (white arrowheads) of the 4A4+ cells (red). Merge panel shows colocalization (yellow). (**G**–**I**) FMRP-IR (green) is present as a thin rim of cytoplasm surrounding the nuclei of mitotic 4A4+ cells (red) dividing at the edge of the lateral ventricle. Merge panel shows colocalization of proteins (yellow). (**J**) Precursor cells in the embryonic subventricular zone express FMRP. FMRP-IR (green) is present in the soma (large arrowhead) and process (small arrowheads) of a 4A4+ cell (red). Cell nuclei are labeled with 4',6-diamidino-2-phenylindole (DAPI) (blue). (**K**) Tbr2+ neural precursor cells (red) in the subventricular zone also express FMRP (green). DAPI staining (blue) confirms Tbr2 nuclear localization (white arrowheads). White dotted line delineates perimeter of the FMRP+ cell. All panels are single optical planes of coronal sections taken on a confocal microscope. Scale bars: (A and B) 100 μm; (C and D) 10 μm; (E–I) 5 μm; (J) 5 μm; (K) 10 μm. White arrows in (J) indicate dorsal (D) and medial (M), and apply to (K).

manner that could impact normal and pathogenic developmental processes in typically developing and premutation individuals, respectively.

Morphology of embryonic neocortical cells appears normal in the premutation mouse

FMRP expression was observed in immature neurons and neural precursor cells in the embryonic neocortex, and since a recent study has shown that hippocampal neurons in young premutation mice display abnormal morphology (32), we examined the morphology of precursor cells and neurons in embryonic premutation mice and wild-type littermates. Heterozygous premutation female mice were crossed with wild-type males to generate littermates that included male and female wild-type embryos and male *Fmr1* premutation embryos. We used 13 wild-type mouse embryos (defined as ~10 CGG repeats) and 14 premutation mouse embryos

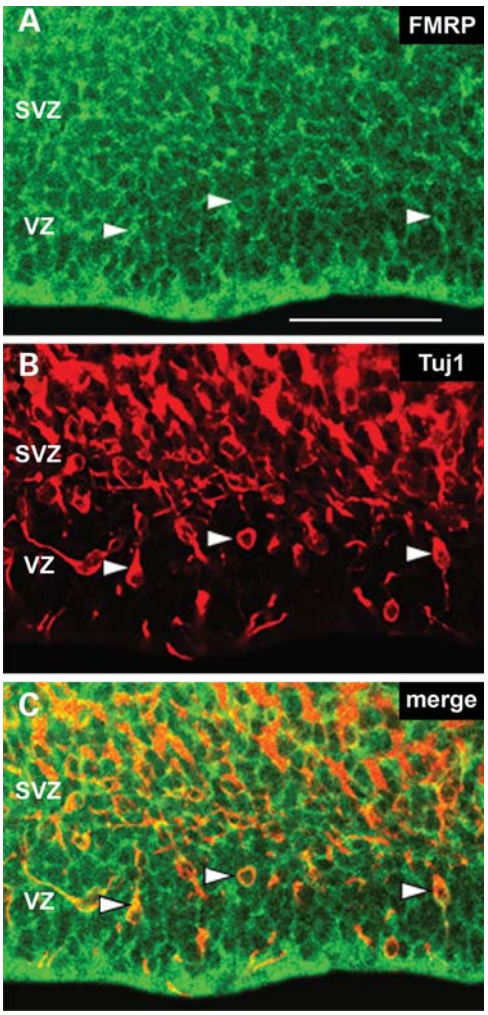

Figure 2. Neuronal cells express FMRP in the embryonic neocortex. (**A**) FMRP immunoreactivity (green) in the ventricular zone (VZ) and subventricular zone (SVZ) of the embryonic neocortex in wild-type E16 mice. (**B**) Tuj1 immunoreactivity (red) labels immature neurons in the same section shown in the top panel. (**C**) Colocalization of FMRP and Tuj1 (yellow). White arrowheads highlight examples of FMRP-expressing Tuj1+ immature neurons in the VZ. Each image is the same single optical plane obtained on a confocal microscope. (A–C) Scale bar = 50 μm.

(~150 CGG) for our analysis. Experimental animals were compared with litter and age-matched wild-type embryos. Precursor cells and immature neurons in the embryonic neocortex were labeled through *in utero* intracerebral injections of a replication incompetent retrovirus encoding enhanced green fluorescent protein (eGFP). This approach labels the entire cell body, cytoplasm and processes of infected embryonic precursor cells and their progeny with the eGFP reporter, permitting detailed studies of the morphology and function of labeled precursor cells and neurons (42,45–49). Three days after *in utero* injection, embryos were sacrificed and perfused intracardially with 4% paraformaldehyde. Coronal sections were prepared from the neocortex of the embryos and eGFP-labeled cells were imaged with a laser-scanning confocal microscope. The genotype, CGG repeat number and gender of embryos were determined through PCR, and embryos were assigned

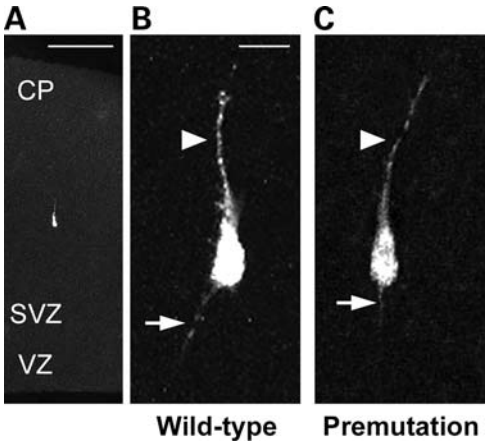

Figure 3. Cells in the embryonic neocortex of premutation mice display normal morphological properties. (**A**) Lower magnification image showing a GFP+ cell migrating toward the cortical plate (CP). (**B** and **C**) Higher magnification image of migrating neurons in the embryonic neocortex of wild-type and premutation mice exhibit the stereotypical tear-drop shape with a leading process (arrowheads) and a short trailing process (arrows). Scale bar: (A) 100 μm, (B–C) 10 μm. VZ, ventricular zone; SVZ, subventricular zone.

to the premutation (~150 CGG repeats) or wild-type (~10 CGG repeats) groups after analysis was completed in a blinded manner.

Embryonic neocortical cells possess a few main processes and do not exhibit complex branching patterns (41,42,45,46,50–52). The morphology of eGFP-labeled radial glial cells and immature neurons in the premutation mice was indistinguishable from that of eGFP-labeled cells in wild-type littermates. Migrating neurons in both groups exhibited a characteristic tear-drop shape (50), with a distinct leading process extending from the soma and a fine trailing process (Fig. 3). The length of the leading process for ventricular and pial directed cells in premutation and wild-type littermates was not significantly different. Leading processes extended 33.0 ± 4.3 μm from the soma in wild-type embryos ($n = 72$ cells) and 29.4 ± 5.7 μm in premutation embryos ($n = 52$ cells). We found no difference in the number of processes elaborated by immature neurons in control brains (1.53 ± 0.35 processes) versus those in the premutation brains (1.57 ± 0.21 processes) ($P = 0.87$; three animals each group, 128 cells analyzed). We also quantified cell size in both groups. Control neurons were slightly larger (168.9 ± 24.2 μm^2) than premutation neurons (146.1 ± 22.1 μm^2), but this difference was not statistically significant ($P = 0.3$; three animals each group, 128 cells analyzed). In addition, the morphology of embryonic neurons in premutation and wild-type mice matched descriptions of embryonic neurons labeled with the eGFP reporter or fluorescent labels in wild-type animals in previous publications (41,42,45,46,51,52). We also compared the thickness of the embryonic neocortex between groups. The thickness of the neocortex was slightly greater in E16 wild-type embryos (578 ± 37 μm) than in E16 premutation mice (557 ± 35 μm), but this difference was not significant ($P = 0.53$; five animals per group). These findings demonstrate that certain aspects of embryonic brain development proceed normally in premutation mice.

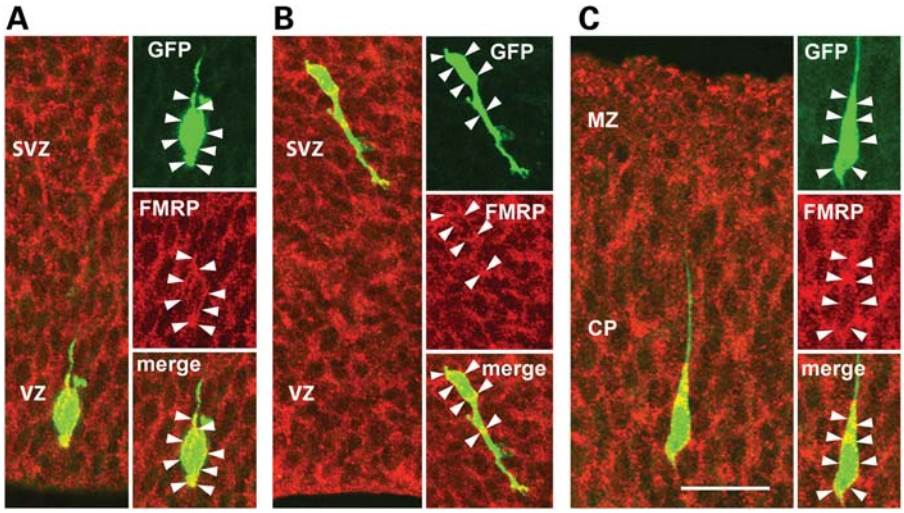

Figure 4. Migrating neurons in the wild-type embryonic neocortex express FMRP. (**A**) A newly born cell near the surface of the lateral ventricle in the ventricular zone (VZ) labeled with a GFP-expressing retrovirus. Panels on the right show the morphology of the GFP-labeled cell (green) and FMRP expression (red), and the merged panel demonstrates colocalization (yellow). (**B**) A ventricular oriented neuron in the subventricular zone (SVZ) labeled with a GFP-expressing retrovirus. Panels on the right show the morphology of the GFP-labeled cell (green) and FMRP expression (red), and the merged panel demonstrates FMRP expression (yellow). (**C**) A neuron migrating radially through the cortical plate (CP) labeled with a GFP-expressing retrovirus. Panels on the right show the morphology of the GFP-labeled cell (green) and FMRP expression (red), and the merged panel demonstrates FMRP expression (yellow). White arrowheads indicate the boundary of the GFP-labeled cells. (A–C) Scale bar = 50 μm. MZ, marginal zone.

Migration of embryonic neocortical cells is impaired in the premutation mouse

We next investigated whether *Fmr1* premutation impacts the migration of neurons in the embryonic neocortex. During gestation, excitatory cortical neurons are produced in the dorsal proliferative zones that line the lateral ventricle. Newborn neurons migrate away from the ventricle along a radial trajectory toward their destination in the overlying CP (50,53), but migrate in distinct stages through a process involving predictable changes in cell morphology and orientation (46). Newborn neurons first migrate to the SVZ where they acquire a multipolar morphology (54), and repeatedly extend and retract multiple processes (46,55,56). The immature neurons then elaborate a single process that extends towards the lateral ventricle and in many cases transiently migrate toward the ventricle (46). Finally, the young neurons extend a new leading process that is directed in the opposite direction toward the overlying CP and commence the radial stage of migration (46,57). We confirmed that the eGFP-labeled migrating cells expressed FMRP during the various stages of migration through FMRP immunostaining (Fig. 4).

The morphology and orientation of retrovirally labeled eGFP+ neurons were quantified and compared between premutation and wild-type embryos. *In utero* retroviral injections were performed on embryos from three pregnant dams at E14 and the embryos were sacrificed 72 h later. The number of CGG repeats and gender of the embryos were determined through PCR and embryos were assigned to groups after analysis was complete. The embryos were perfused with 4% paraformaldehyde and sectioned coronally on a vibratome. Freely migrating cells were imaged on a confocal microscope and were classified by their orientation with respect to the ventricular surface in a blinded fashion as either: (i) directed toward the VZ; (ii) directed toward the pia; or (iii) no clear orientation/multipolar (Fig. 5A–C). This classification scheme included greater than 98% of the freely migrating eGFP-labeled cells in the experimental and control brains (three embryos per group, $n = 309$ cells). The remaining cells could not be classified and were excluded from further analysis. In wild-type mice, roughly 18% of the migrating cells were oriented toward the ventricle; 40% were multipolar with no clear orientation and the remaining 42% were oriented toward the pia. In contrast, in the premutation mice, approximately 7% of the migrating cells were oriented toward the ventricle; approximately 43% were multipolar with no clear orientation and approximately 50% were oriented toward the pia. The number of cells classified in each of the three categories was compared between the premutation and wild-type embryos and found to be significantly different ($\chi^2 = 7.35$; d.f. = 2; $P < 0.03$, see Fig. 5D). The proportion of labeled cells that were oriented towards the ventricle was also significantly different between groups: fewer cells were oriented toward the ventricle in the premutation group ($P < 0.01$, *t*-test). Thus, cortical neurons in premutation mice displayed a subtle yet significantly different orientation compared with cortical neurons in wild-type littermates. Relevant variables were controlled in these experiments including time of mating, date of retroviral injection, gestational day when the retroviral injections were performed (E14.0), length of time between retroviral injection and embryo sacrifice (72 h) and the region of the brain analyzed (dorsolateral somatosensory cortex). These results are consistent with the hypothesis that premutation of the *Fmr1* gene is associated with a disturbance in the normal pattern of neuronal migration in the embryonic neocortex.

Since migrating cells displayed an abnormal orientation in the neocortex of premutation mice, we tested whether the eGFP cells migrated toward their appropriate destination. The distribution of eGFP+ migrating cells was compared in the embryonic

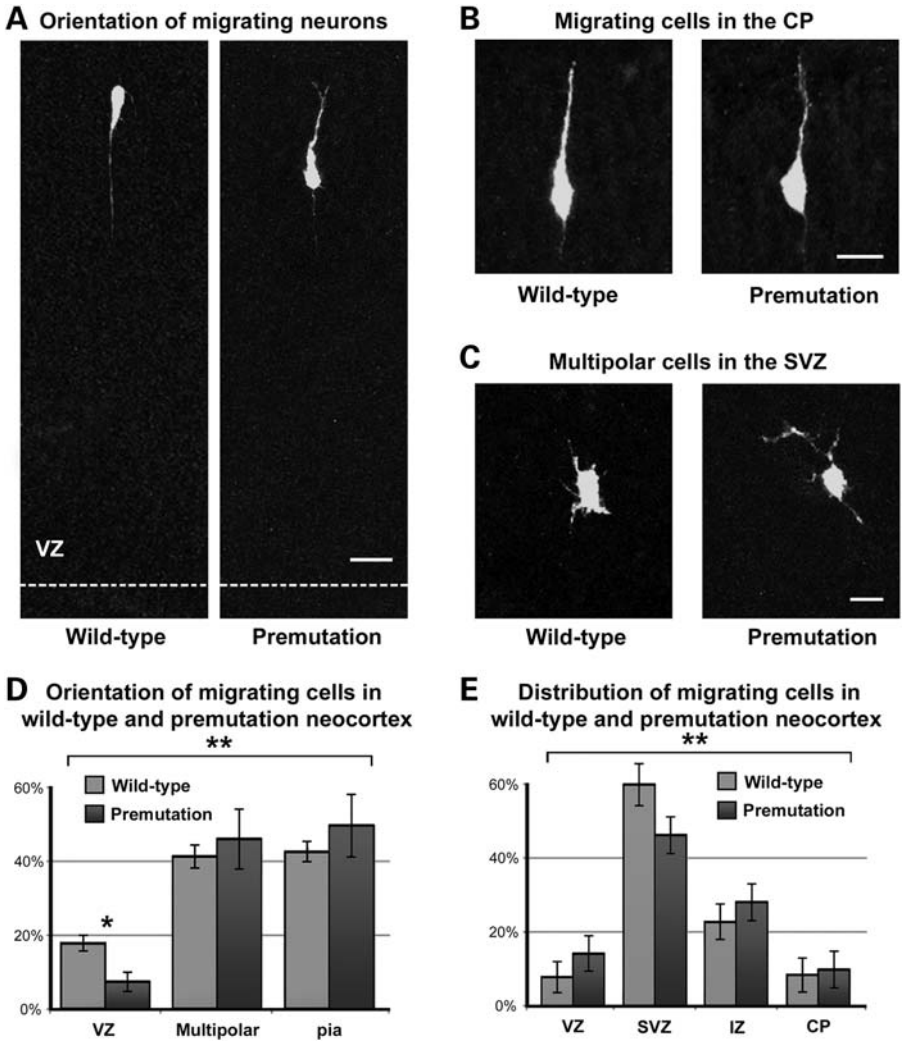

Figure 5. The orientation and distribution of migrating neurons are altered in the embryonic neocortex of premutation mice. (**A**) GFP-expressing cells in the embryonic neocortex of wild-type and premutation mice. Fewer migrating cells are oriented toward the ventricular zone (VZ) in the premutation mice compared with wild-type controls. White dotted line indicates the margin of the lateral ventricle. (**B**) Examples of migrating cells in the cortical plate of premutation and wild-type mice. (**C**) A similar proportion of cells exhibited a multipolar morphology in the subventricular zone of wild-type and premutation mice. (**D**) Histogram displaying the proportion of migrating GFP-labeled cells in wild-type mice (light grey bars) and premutation mice (dark grey bars) that are oriented toward the ventricular zone (VZ), that are oriented toward the pia or that have no discernible orientation (multipolar). Fewer cells are oriented toward the ventricle in the premutation group, and similar proportions of cells are multipolar or oriented toward the pia in each group. A Chi-square test shows a significant difference between groups ($\chi^2 = 7.35$; d.f. $= 2$; $P < 0.03$, double asterisk), and a *t*-test shows that fewer GFP-labeled cells are oriented toward the ventricle in the premutation group ($P < 0.01$, asterisk). (**E**) The distribution of GFP+ migrating cells in premutation mice differs from wild-type controls. Fewer GFP+ cells were located in the SVZ of premutation mice. A Chi-square test shows a significant difference between premutation and wild-type embryos ($\chi^2 = 10.06$; d.f. $= 3$; $P = 0.018$, double asterisk). Error bars show SEM. Scale bar: (A) 25 μm; (B) 10 μm; (C) 10 μm.

neocortex of premutation and wild-type mice. The number of GFP+ migrating cells located in the VZ, SVZ, IZ or CP was quantified in each group and found to be significantly different ($\chi^2 = 10.06$; d.f. $= 3$; $P = 0.018$). There were more GFP+ cells located in the SVZ of wild-type mice and a slight but not significant increase in the number of GFP+ cells located in the IZ, CP and VZ of premutation mice (Fig. 5E).

Differentiation of embryonic neocortical cells is altered in premutation mice

Embryonic cells in the neuronal lineage progress along a differentiation pathway that is marked by sequential changes in the expression of transcription factors. To examine the differentiation of neocortical cells in premutation mice, we immunostained coronal sections of the neocortex obtained from premutation mice and wild-type littermates at E16 with antibodies that label transcription factors specific to distinct populations of embryonic neural precursor cells. Radial glial cells in the VZ express the transcription factor Pax6, and intermediate progenitor cells in the SVZ express the transcription factor Tbr2 (58). The number of cells that expressed Pax6 or Tbr2 was quantified in 200 μm wide bins that stretched from the ventricle to the pial surface in the dorsal neocortex of five premutation and five wild-type mice. The number of cells that expressed the transcription factor Pax6 was

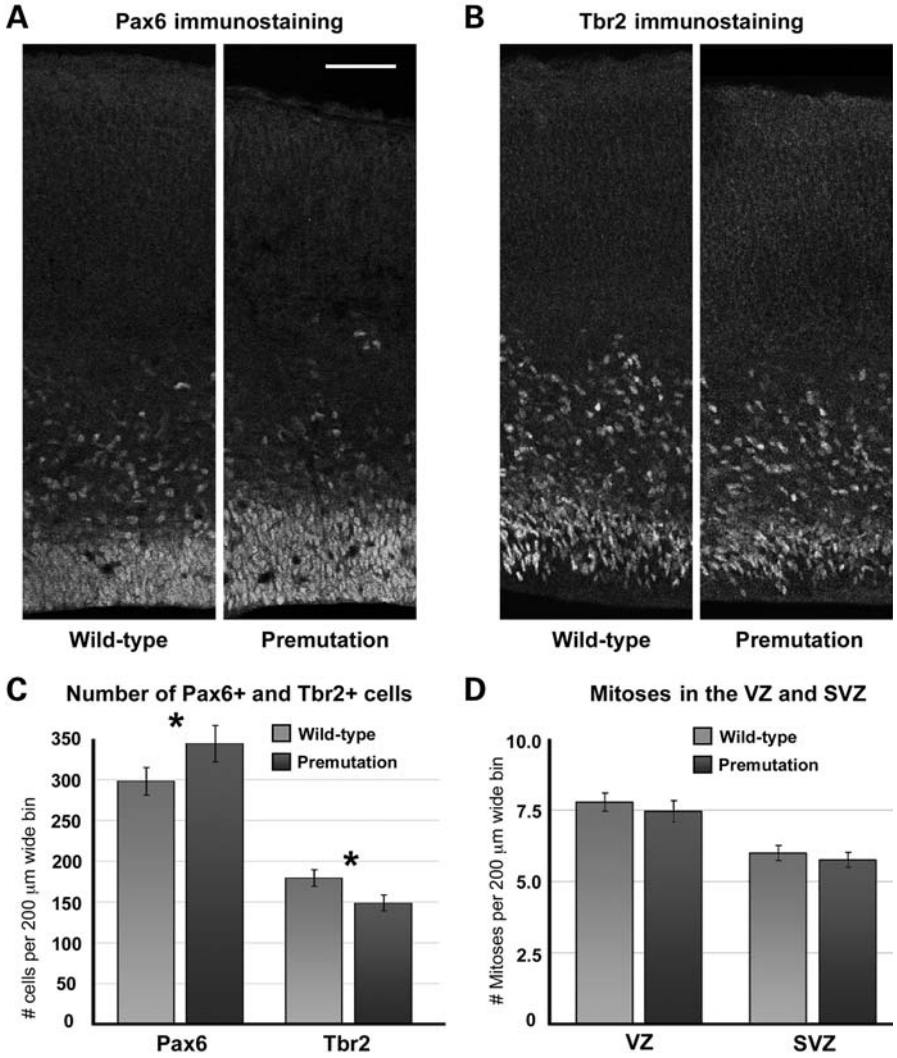

Figure 6. Expression of the transcription factors Pax6 and Tbr2 is altered in embryonic premutation neocortex. (**A**) Pax6 is expressed by precursor cells in the embryonic ventricular zone (VZ). Pax6+ cells in wild-type and premutation mice are displayed in 200 μm wide radial sections of neocortex that span from the ventricle to the pial surface. (**B**) Tbr2 is expressed by neural precursor cells in the embryonic subventricular zone (SVZ). Tbr2+ cells in wild-type and premutation mice are displayed in 200 μm wide radial sections as described above. (**C**) The number of Pax6+ cells is significantly increased by 15% in premutation mice ($P < 0.05$, asterisk). In contrast, the number of Tbr2+ cells is significantly reduced by 17% in the premutation mice ($P < 0.05$, asterisk). (**D**) The change in Pax6+ and Tbr2+ cell numbers is not produced by an alteration in proliferation. The number of 4A4+ mitoses does not differ in the VZ or the SVZ of wild-type (light grey) and premutation (dark grey) littermates. Error bars show SEM. (A–B) Scale bar = 50 μm.

approximately 15% greater in the premutation neocortex: 298.2 ± 17.6 Pax6+ cells per 200 μm bin in the wild-type neocortex versus 345.2 ± 40.9 Pax6+ cells per 200 μm bin in the premutation embryos (five embryos per group, 19 730 cells, Fig. 6A and C). Comparison of the means revealed a statistically significant difference between groups ($P < 0.05$, Student's *t*-test). In addition, the number of neocortical cells that expressed the transcription factor Tbr2 was approximately 17% lower in premutation mice: 179.4 ± 10.1 Tbr2+ cells per 200 μm bin in the wild-type neocortex and 149.0 ± 9.9 Tbr2+ cells per 200 μm bin in the premutation neocortex (five embryos per group, 4,598 cells, Fig. 6B and C). Comparison of the means revealed a statistically significant difference between groups ($P < 0.05$, Student's *t*-test).

Alterations in several developmental parameters could increase the number of Pax6+ cells and decrease the number of Tbr2 cells in the embryonic premutation neocortex, including increased proliferation of Pax6 cells, decreased proliferation of Tbr2 cells and/or increased cell death among Tbr2 cells. To test for these possibilities, we first quantified and compared the level of proliferation in the embryonic neocortex of premutation and wild-type mice. Coronal sections of the embryonic E16 neocortex were immunostained with the 4A4 antibody, which labels all mitotic precursor cells in the embryonic neocortex (41) and counterstained with the DAPI nuclear marker. 4A4+ or DAPI mitotic cells were counted in 200 μm wide bins of the dorsal somatosensory neocortex that stretched from the ventricle to the pia. Analysis included mitotic cells at the ventricular surface, which represent Pax6+ radial glial cell divisions, and mitotic cells away from the ventricle, which represent Tbr2+ intermediate progenitor cells in the SVZ (59). The total number of mitotic cells (4A4+ or

DAPI) did not differ between groups. Furthermore, the number of ventricular mitoses and the number of abventricular mitoses did not differ between groups (five embryos per group, 384 4A4+ cells, 464 DAPI cells, Fig. 6D and Supplementary Material, Fig. S1). This result suggests that increased numbers of Pax6 cells and decreased numbers of Tbr2 cells in the premutation neocortex did not result from altered proliferation. Since *FMR1* premutation is associated with Purkinje cell degeneration (60) and since viability of premutation hippocampal neurons is reduced after 3 weeks in culture (32), we tested whether there was an increase in cell death in the premutation neocortex. A TUNEL reaction was performed on neocortical tissue prepared from E16 premutation and wild-type mice to label apoptotic and necrotic cells. The number of TUNEL+ cells was quantified in the dorsolateral somatosensory neocortex and no difference was observed between groups (three embryos per group, 509 cells, Supplementary Material, Fig. S2). This indicates that increased cell death did not decrease the number of Tbr2 cells in the premutation mice. Since the premutation embryos were males and wild-type embryos included males and females in our experiments, we investigated whether gender impacts the developmental processes under study. The level of proliferation was compared across gender and no significant differences were found in the number of DAPI mitoses in wild-type males versus wild-type females (data not shown). Together, these data indicate that other mechanisms that influence cellular differentiation are responsible for the change in Pax6+ and Tbr2+ cell numbers. Indeed, the total number of Pax6+ cells plus Tbr2+ cells per embryo in wild-type and premutation littermates did not differ between groups (448.1 $\pm$ 26.0 cells in wild-type embryos versus 488.4 $\pm$ 37.3 in premutation embryos), suggesting that delayed differentiation of the Pax6+ cell population in the premutation neocortex may have produced a shift in cell numbers toward more Pax6+ cells and fewer Tbr2+ cells.

FMRP expression is reduced in the embryonic neocortex of premutation mice

Previous publications have found that FMRP levels are reduced in lymphocytes obtained from juveniles and adults with the *FMR1* premutation (20,61) and in homogenates prepared from whole brains of adult premutation mice (29). To explore whether the level of FMRP expression was reduced in the neocortex of embryonic premutation mice, we analyzed the comparative level of FMRP expression in the embryonic telencephalon in wild-type and premutation mice through SDS–PAGE followed by western blotting. The ratio of FMRP expression to the loading standard beta-actin was reduced in the premutation embryonic telencephalon by 42% compared with wild-type (Fig. 7). Since previous reports have described the presence of intranuclear inclusions in neurons and glial cells in the cerebral cortex of human *FMR1* premutation and the premutation mice (16,24,31), we tested whether intranuclear inclusions were present in the embryonic neocortex. Cortical tissue was stained with anti-ubiquitin antibodies, but no evidence for ubiquitin+ inclusions in the embryonic neocortex was found. This suggests that inclusion formation does not begin in premutation mice before birth, consistent with previous reports that found few inclusions in premutation mice younger than 12 weeks of age (31) and in neurons cultured from postnatal day 1 premutation mice (32).

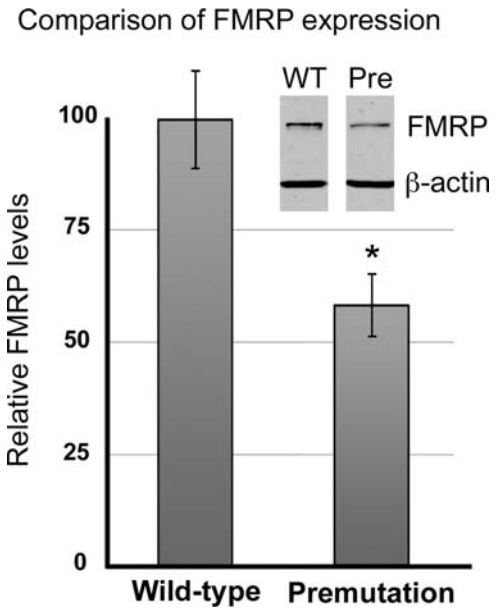

Figure 7. FMRP levels in the telencephalon of premutation embryos (six embryos, 94–167 CGGs) compared with wild-type embryos (three embryos, 9–15 CGGs). Histograms display the ratio of densitometric measurement of FMRP-IR bands corrected to the loading standard beta-actin-IR bands. Premutation mice show a reduced level of FMRP that is approximately 58% of wild-type levels ($P < 0.05$, asterisk). Inset shows two representative samples. Error bars show SEM.

DISCUSSION

In the present study, we tested whether the *Fmr1* premutation impacts brain development during gestation. We show that neuronal migration is impaired in embryonic premutation mice. Migrating neurons in the embryonic premutation neocortex exhibit an altered orientation and distribution in comparison to controls. We also show that the expression of transcription factors that identify VZ and SVZ precursor cells is altered in premutation mice. Finally, we show that FMRP expression is slightly reduced in the embryonic brain. Together these results support the hypothesis that *FMR1* premutation impacts prenatal brain development.

FMRP is expressed by neural precursor cells and neurons in the embryonic neocortex

We show strong FMRP expression in the embryonic CP, in migrating neurons and in proliferative precursor cells in the embryonic neocortex of wild-type mice (Fig. 1). Expression of *FMR1* mRNA and FMRP in the developing prenatal brain has been reported in previous studies. Abitbol *et al.* (33) labeled the human telencephalon with probes against *FMR1* mRNA and reported strong expression in the proliferative zones and in immature cells with the apparent morphology of migrating neurons at 8 and 25 weeks of gestation (33).

FMRP expression has been shown in the fetal human (34), and rodent neocortex (35), with marked expression in the proliferative zone at the edge of the ventricle (35). Our immunohistochemical results confirm these previous findings and demonstrate that altered *FMR1* mRNA and/or FMRP expression could impact a wide range of developmental programs in the prenatal brain. Examination of human neocortical tissue from premutation subjects with FXTAS has not revealed gross pathological defects (16), and our data indicate that the embryonic premutation neocortex is not significantly thinner than wild-type cortex. Despite the lack of gross pathological findings in FXTAS or mouse premutation brains, recent studies have provided compelling evidence to suggest that *FMR1*/*Fmr1* premutation is associated with abnormalities in the morphology and/or function of neurons in the developing brain. Children with the *FMR1* premutation are more likely to suffer from psychological symptoms, ADHD and autism spectrum disorders (3,36,37,62,63), and recent work shows that hippocampal neurons obtained from *Fmr1* premutation mice shortly after birth and grown in culture display abnormalities in dendritic morphology and synapse formation (32). Together, these findings support the concept that *FMR1* premutation impacts embryonic developmental programs.

Fmr1 premutation is associated with a migration defect in the embryonic neocortex

We find that the migration of cortical neurons is impaired in embryonic *Fmr1* premutation mice. Neuronal migration relies upon cellular interactions with extrinsic signals and intracellular mechanisms that drive the elaboration of filopodia or leading processes. Time-lapse studies show that migrating neocortical neurons explore their local environment by extending multiple filopodia or processes to probe the surrounding environment, especially when the migrating cells are located in the SVZ (46,55,56,64). The migration of cortical neurons does not proceed along a straight trajectory, but instead involves multiple stages that can be identified based on the morphology and orientation of the migrating cell (46). Our data show that migrating neurons in the premutation neocortex display an altered orientation and distribution in comparison to their wild-type littermates. Fewer cells in the premutation mice were oriented toward the ventricle (Fig. 5D), and fewer cells were located in the SVZ (Fig. 5E). The significance of changes in orientation during migration has not been determined, but the behavior of migrating cells in the wild-type cortex suggests that the migratory pause in the SVZ provides neurons with appropriate signals that direct radial migration and perhaps the development of synaptic connectivity (65). During migration, many neocortical neurons pause in the SVZ for periods of 1 day or longer before resuming radial migration toward the CP (46,66). The immature neurons in the SVZ acquire a multipolar morphology as they extend and retract multiple processes in a manner that suggests a search for environmental cues (46,55). Fewer GFP-labeled cells were located in the SVZ of premutation mice, indicating that immature neurons in the premutation mice spend less time in the SVZ compared with wild-type neurons. This suggests that premutation neurons may not receive or correctly process the same extrinsic signals as wild-type neurons in the SVZ. This abnormal signaling could play a role in the altered orientation of premutation neurons during embryonic development and could impact connectivity of the cortical neurons later during development. The impaired ability of immature neurons to extend dendrites in premutation mice (32) may be associated with the migration defect we observed in the embryonic premutation mice since common signaling pathways are involved in neuronal migration and dendritic process extension in some cases. For example, the protein semaphorin 3A regulates both the radial migration of cortical neurons (67) and the elaboration of new dendrites by cortical neurons (68,69). Thus, if the *Fmr1* premutation interrupts only one signaling pathway in young neurons, it could nonetheless impact multiple processes in the developing brain.

Despite the disturbance in orientation and distribution we observe in the embryonic premutation mice, evidence from adult FXTAS subjects showing a lack of gross cortical neuropathology (16) suggests that cortical neurons may ultimately reach their target destination. Nonetheless, the subtle change in distribution of immature neurons in the premutation mice could alter patterns of cell–cell contact that are thought to presage neuronal connectivity (70), which could subsequently alter cognitive functioning. While migrating neurons in the premutation and control mice exhibited differences in orientation and distribution, the migration of many neurons in the premutation neocortex appeared indistinguishable from that in wild-type brains. Thus, the *Fmr1* premutation may primarily affect a subpopulation of migrating cells. Evidence suggests that as few as 5% of neocortical neurons in FXTAS patients display the intranuclear inclusions that are a hallmark of *FMR1* premutation neuropathology (16), and the proportion of neurons that exhibit intranuclear inclusions in the premutation mouse parallels results from human subjects (29,31). These results support the idea that the *FMR1*/*Fmr1* premutation impacts a subpopulation of cortical neurons. Accumulating evidence suggests that migration defects are associated with autism spectrum disorders (71), and the presence of autism among premutation carriers suggests that premutation-associated RNA toxicity (10,60) may also extend to early developmental dysregulation involving altered neuronal migration. Furthermore, periventricular nodular heterotopia has been reported in the brains of FXS subjects who lack FMRP (72), which suggests that FMRP may also play a role in neuronal migration. Our data showing a decrease in FMRP expression in premutation mice (Fig. 7) and abnormal patterns of neuronal migration in *Fmr1* premutation mice (Fig. 5) are consistent with this idea. These findings suggest that further examination of neocortical tissue from subjects with *FMR1* premutation alleles is warranted.

Differentiation of neocortical neurons is altered in the premutation neocortex

We find a significant increase in the number of cortical cells that express the Pax6 transcription factor and a significant decrease in the number of cells that express the Tbr2 transcription factor in embryonic premutation mice. These alterations were not likely the result of increased proliferation or cell death during prenatal cortical development since the number

of mitotic cells and apoptotic cells did not differ between groups (Fig. 6D and Supplementary Material, Fig. 2). Ablation of Tbr2 expression in the embryonic rodent neocortex produces a vast reduction in the level of proliferation and in the number of cortical neurons produced (73). We find a 17% reduction in the number of cells that express Tbr2 in the premutation neocortex, which is apparently not sufficient to produce a measureable decrease in cortical proliferation. A recent study by Tervonen *et al.* (74) reported increased Tbr2 expression in embryonic *Fmr1* KO mice. However, that study reported increased Tbr2 expression at E17, but not at E16, the gestational age at which we found decreased Tbr2 expression. The difference in findings between our study and that of Tervonen *et al.* (74) likely result from the different mouse models under study. The *Fmr1* KO does not express *Fmr1* mRNA with elevated CGG repeats, which are expressed in the premutation mice, nor does it express FMRP, which is also present in the premutation mice. A comparison of these studies suggests that expression of expanded CGG repeats in the *Fmr1* gene may underlie the altered number of Pax6 and Tbr2 expressing cells in premutation mice. However, it should be noted that the increased number of Pax6-expressing cells we observed could have impacted the number of Tbr2-expressing cells. Pax6-expressing radial glial cells produce Tbr2-expressing precursor cells (58). *Fmr1* premutation may alter precursor cell numbers by producing a delay in the differentiation of Pax6-expressing cells, which could be expected to increase the number of Pax6+ cells at the expense of Tbr2+ cell numbers. This apparent change in precursor cell fate may represent a delay that is resolved at later stages of development, but could nonetheless impact the functional properties of cortical cells produced during prenatal development. Decreased Tbr2 expression itself may contribute to the migration abnormalities observed in the premutation mice. Tbr2 acts to inhibit cell cycle exit (73), and it also regulates the migration of GABAergic neurons (75) and epiblast cells (76). Tbr2 is thought to down-regulate the expression of cell adhesion molecules (76), thereby freeing migratory cells to move toward their destination. Decreased Tbr2 expression in premutation mice may therefore interfere with the ability of cortical neurons to regulate adherence with their migratory substrate, contributing to the altered orientation of migrating cells in the *Fmr1* premutation brain.

Functional implications of *Fmr1* premutation

Premutation expansion of CGG repeats in the *Fmr1* gene may impact neuronal development and function through several mechanisms. The level of *FMR1*/*Fmr1* mRNA is elevated in both human premutation carriers (20,77) and premutation mice (28,29,78). The number of CGG repeats is correlated with the level of mRNA expression and the number of intranuclear inclusions (16,20). These findings support the RNA toxicity model of FXTAS (60,79,80), which suggests that the elevated level of *FMR1* mRNA is responsible for inducing the characteristic cellular changes associated with premutation. It has yet to be determined whether increased levels of *FMR1* mRNA produces cytotoxicity, or rather if increased lengths of the CGG trinucleotide repeat is sufficient to initiate premutation dysfunction. Recent work by Arocena *et al.* (26) supports the latter hypothesis. Cultured neural progenitor cells transfected with a plasmid encoding a CGG_{88} repeat induced cellular changes similar to those described in the *Fmr1* premutation mice, including intranuclear inclusions. Furthermore, Hashem *et al.* (27) found that induced expression of a CGG_{90} repeat in Purkinje neurons produced intranuclear inclusions, neurodegeneration and motor deficits similar to those found in FXTAS. Expanded CGG repeats form large intranuclear RNA aggregates that recruit RNA binding proteins such as the splicing-regulatory protein Sam68 in both the mouse premutation model and also in FXTAS patients (81). The sequestered Sam68 thereby loses its regulatory function. In addition to splice regulation, Sam68 also plays a role in developmental processes that include cell migration (82). Expanded trinucleotide repeats in other genes also exert cytotoxic effects. For example, an expanded CUG repeat in the *DMPK* gene is thought to exert cytotoxic effects through non-coding trinucleotide transcripts that sequester proteins and impair RNA transcription, splicing and export to produce the cellular dysfunction associated with myotonic dystrophy (83).

Premutation alleles of *FMR1*/*Fmr1* can also reduce the level of FMRP protein (20,29,61). FMRP is a selective RNA binding protein that binds up to 4% of total mouse brain mRNAs (84). Absence of FMRP in *Fmr1* KO mice or in FXS may lead to abnormally high levels of translation for FMRP-associated mRNAs (85). Furthermore, FMRP interacts with a number of mRNAs including Semaphorin 3F (86), which is important for axon pathfinding (87), and has also been shown to regulate neuronal migration in some model systems (88). Our results indicate that FMRP expression is reduced in the embryonic premutation neocortex by approximately 42%. Thus, decreased levels of the FMRP may play a modifying role in the phenotype we describe in the embryonic premutation neocortex. Recent publications have reported that FMRP plays a role in the regulation of precursor cell proliferation and differentiation in the adult murine brain (89) and in *Drosophila* (90). However, in the present study, we did not observe a change in proliferation in premutation mice that have reduced levels of FMRP. This suggests either that FMRP plays a significant regulatory role only in adult precursor cells or perhaps that since FMRP expression is reduced, but not silenced, in the embryonic premutation mice (Fig. 7), its function is retained and proliferation not measurably disturbed. The distinct contributions of mRNA overexpression and reduced FMRP expression to the premutation phenotype remain to be differentiated. Nonetheless, the present findings provide strong evidence that downstream effects of the *Fmr1* premutation are present in the prenatal brain.

Conclusions and clinical implications

We show that *Fmr1* premutation is associated with developmental impairments in the embryonic neocortex. We show that: (i) FMRP is expressed in the neocortex by mitotic precursor cells and migrating neurons in the normal embryonic mouse; (ii) neural migration is impaired in the embryonic cerebral cortex of premutation mice; (iii) there is a significant change in the number of cells in embryonic premutation mice that express the transcription factors Pax6 and Tbr2;

and (iv) FMRP expression is reduced in the embryonic brain of premutation mice. Premutation alleles of the *FMR1* gene produce distinct clinical and pathological outcomes that are dependent on length of the CGG repeat in the gene. The present results obtained from premutation mice with CGG_{150} repeats are consistent with the hypothesis that cytotoxic levels of *Fmr1* mRNA containing CGG repeats, possibly in combination with decreased levels of FMRP, produce developmental deficits in the cerebral cortex. These data suggest that the *FMR1* premutation allele impacts the developing brain during gestation, earlier than previously realized. With recent advances in the detection of *FMR1* premutation (91), it may be feasible to identify those at risk prior to birth, and to explore treatment strategies that are appropriate for infant carriers of the premutation.

MATERIALS AND METHODS

Animals

The expanded CGG trinucleotide repeat knock-in mouse model of the Fragile X premutation (referred to as premutation mouse) was generated and described previously (28,92). Briefly, a region of the 5′-UTR of the mouse *Fmr1* gene that contains approximately eight CGG trinucleotide repeats was replaced with a length of 98 CGG repeats of human origin by homologous recombination. This region of CGG trinucleotide repeats demonstrated mild instability with contractions and expansions of the number of CGG repeats occurring across breedings. Animals were only examined if the number of CGG repeats was within the Fragile X premutation range, defined as between 55 and 200 CGG repeats (28,29). Heterozygous premutation female mice were crossed with wild-type males to generate litters consisting of wild-type males and females, heterozygous females and premutation male embryos. Embryos were manipulated, and genotyping was performed *post hoc*. We used 13 wild-type mouse embryos (defined as ∼10 CGG repeats) and 14 premutation mouse embryos (∼150 CGG) for our analyses. All experimental animals were compared with age-matched wild-type littermates. Premutation breeders and pregnant mice were housed under a 12/12 h light–dark cycle with food and water ad lib. All experiments were conducted in compliance with the NIH Guide for Care and Use of Laboratory Animals and were approved by the Institutional Animal Care and Use Committee of the University of California at Davis.

Genotyping

DNA was extracted from embryonic mouse tails by incubating with 10 mg/ml Proteinase K (Roche Diagnostics) in 300 μl lysis buffer containing 50 mM Tris–HCl, pH 7.5, 10 mM EDTA, 150 mM NaCl and 1% SDS overnight at 55°C. One hundred microliters of saturated NaCl were then added and the suspension was centrifuged. One volume of 100% ethanol was added, gently mixed, the DNA was pelleted by centrifugation and the supernatant discarded. The DNA was washed and centrifuged in 500 μl of 70% ethanol. The DNA was then dissolved in 100 μl double-distilled water (MilliQ-H_2O). The numbers of CGG trinucleotide repeats for the wild-type and premutation embryos were characterized by PCR using the Expanded High Fidelity Plus PCR System (Roche Diagnostics). Briefly, approximately 500–700 ng of DNA was added to 50 μl of PCR mixture containing 2.0 μM of each primer, 2% PCR Grade DMSO (Sigma), 25 mM dNTP mix (Fermentas), 5 M Betaine (Sigma), 10 μl 5X Expand High Fidelity Plus Buffer with Mg (Roche) and 1 μl of Expand High Fidelity Plus PCR System Enzyme (Roche). The forward primer used was 5′-CGGAGGCGCCGCTG CCAGG-3′ and the reverse primer was 5′-TGCGGGCG CTCGAGGCCCAG-3′. The PCR reaction commenced with a 10 min denaturation at 95°C, followed by a program (repeated for 34 cycles) that included denaturation for 1 min at 95°C, annealing for 1 min at 65°C, and elongation for 5 min at 75°C. The PCR reaction ended with a final elongation step of 10 min at 75°C. DNA CGG band sizes were determined by running DNA samples on a 2.5% agarose gel and staining DNA with ethidium bromide. For gender analysis, DNA was extracted from embryonic mouse tails as above and gender determined by using Platinum PCR Supermix (Invitrogen). Briefly, 1 μl of DNA was combined with 1 μl of each primer for a final concentration of 200 nM along with 10 μl of Platinum PCR Supermix. The primers used originated from the exon coding for Sry protein. The forward primers used were Sry-1 5′-TGGGACTGGTGACAATTG TC-3′ and IL3-1 5′-GGGACTCCAAGCTTCAATCA-3′. The reverse primers used were Sry-2 5′-GAGTACAGGTGTG CAGCTCT-3′ and Il3-2 5′-TGGAGGAGGAAGAAAAG CAA-3′.

Preparation of retrovirus

Replication-incompetent pantropic retrovirus encoding the eGFP reporter gene pseudotyped with the vesicular stomatitis virus (VSV)-G glycoprotein was produced from the 293gp NIT-GFP stably transfected packaging cell line (generous gift of Drs Fred Gage and Theo Palmer). Briefly, cells from the packaging line were cultured to ∼90% confluence and transiently transfected with pVSV-G. Supernatant was collected from cells at 48–72 h post-transfection, centrifuged and viral particles were concentrated, collected and stored at −80°C until use. The retroviral construct was engineered to be replication incompetent, to instruct host cells to express eGFP protein (driven by the cytomegalovirus promoter) rather than retroviral proteins (93) and was pseudotyped to initiate virus entry into mammalian cells through interaction with ubiquitous membrane elements (94).

Animal surgery

Timed pregnant mice were anesthetized with 5% isoflurane, a laparotomy was performed and the uterine horns were removed. For experiments involving GFP-expressing retrovirus, *in utero* intracerebral injection of low titer retrovirus (1×10^5 cfu/ml) into the lateral ventricles as described previously (45) was performed on E14 mouse embryos. Introducing low titer retrovirus into the lateral ventricle reduced the likelihood that the processes of the eGFP-labeled cells under study would overlap those of other nearby eGFP-labeled cells, allowing us to study the morphology of eGFP+ cells

in fine detail (42,45,46). After injection, the peritoneal cavity was lavaged with warm artificial cerebrospinal fluid the uterine horns were replaced and the wound was closed. After the surgery, pregnant animals were monitored and given buprenophine (0.5 mg/kg) as an analgesic. The embryos were allowed to survive for 3 days, after which they were removed, tails clipped for genotyping and transcardially perfused with 4% paraformaldehyde. Animal surgeries were approved by the Institutional Animal Care and Use Committee of the University of California at Davis.

General tissue preparation

Embryos resulting from premutation matings were removed from anesthetized pregnant females, the tails were clipped for genotyping and the embryos were transcardially perfused with 4% paraformaldehyde. Brains were removed, post-fixed for 2 h in 4% paraformaldehyde and cryoprotected overnight in 30% sucrose. Cryoprotected brains were stored at −80°C until they were sectioned at 30 μm on a cryostat (Microm) or at 300 μm on a vibratome (Ted Pella) and mounted on glass slides or floated in 24 well plates.

Immunohistochemistry

Embryos were removed, fixed and cryostat/vibratome sectioned and mounted on glass slides or collected in 24 well plates as above. Antigen retrieval was performed by boiling sections for 15 min in 10 mM citrate buffer (pH 6.0) in a microwave. Endogenous peroxidase (for immunoperoxidase reactions) was quenched by incubating sections in 0.3% H_2O_2 for 30 min. Sections were incubated in blocking buffer that contained 10% donkey serum, 0.1% Triton X-100 and 0.2% gelatin for 1 h at RT. Sections were then incubated overnight at RT in primary antibody buffer containing 2% donkey serum, 0.02% Triton X-100 and 0.04% gelatin and primary antibodies that included mouse anti-4a4 1:1000 (MBL Intl), mouse anti-FMRP 1:200 (clone 1C3, Millipore), rabbit anti-Tbr2 1:1000 (Abcam), mouse anti-Pax6 supernatant 1:1 (DSHB), rabbit anti-Pax6 1:150 (Covance), mouse anti-Tuj1, 1:1000 (Covance), and/or chicken anti-FMRP, 1:2000 for immunofluorescent reactions, 1:20 000 for immunoenzymatic reactions (38). For immunofluorescence, sections were rinsed and incubated in fluorescent conjugated donkey anti-mouse (1:200), donkey anti-rabbit (1:200) or donkey anti-chicken (1:200) secondary antibodies (Jackson Labs) for 1–2 h at RT. Sections were rinsed, incubated in DAPI (1:1000) for 10 min and mounted in Mowiol. For DAB immunoperoxidase reactions, sections were rinsed and incubated in biotin-conjugated goat anti-chicken (1:200) secondary antibodies (Vector) for 1 h. Sections were rinsed and the immunoenzymatic reaction was visualized with an ABC horseradish peroxidase kit using DAB or Nova Red (Vector) as the chromagen. Sections were dehydrated in consecutive 5 min ethanol treatments of 50, 75, 95 and 100% EtOH treated with two 15 min periods of Safeclear (Fisher) and mounted. Positive controls for chicken anti-FMRP antibody were performed by comparing embryonic staining patterns to those obtained in the cerebral cortex and hippocampus of tissue from postnatal wild-type animals. Negative controls for chicken anti-FMRP included omission of the primary antibody, immunostaining of embryonic and adult *Fmr1* KO neocortical tissue, and incubation of wild-type embryonic cortical tissue with preimmune serum at 1:1 and 1:2000 in place of the primary antibody.

Confocal microscopy

Slices were viewed and imaged on a Fluoview FV1000 Confocal Microscope (Olympus). Single optical planes were used for analysis of co-expression. Analysis and quantification were performed on the Olympus software and in Photoshop CS3 (Adobe). Images were cropped, contrast adjusted and false color applied in Photoshop.

Morphological analysis of retrovirally labeled cells

After retroviral injection and later perfusion, brains from premutation and wild-type mice were sectioned at 300 μm on a vibratome and equivalent, age-matched sections from three premutation and three wild-type mice were compared. The three premutation mice were male, and two of the three wild-type embryos were female. We tested for gender differences and found none (see proliferation analysis below). All cells that expressed GFP in the developing dorsal cortical wall were imaged on an Olympus FV1000 confocal microscope. The orientation of migrating cells were analyzed with reference to the ventricular surface and categorized as either: (i) oriented toward the ventricle; (ii) oriented toward the pia; or (iii) multipolar with no clear orientation. Distribution of cells (located in VZ, SVZ, IZ or CP), polarity (unipolar, bipolar or multipolar) and expression of Tbr2 were also noted for each cell.

Pax6 and Tbr2 analysis

To determine whether the number of cells expressing the radial glial marker Pax6 or the intermediate progenitor cell marker Tbr2 differed between premutation mice and wild-type embryos, coronal sections were immunostained and imaged on a confocal microscope as described above. Bins 200 μm wide that stretched from the ventricular surface to the pial surface of the embryonic brain were created. One bin was created for each hemisphere in the coronal sections. All Pax6- or Tbr2-positive cells in the bin in a single optical plane were counted. Results were averaged from three coronal sections per embryo. Comparable rostrocaudal and dorsoventral regions of somatosensory cortex were analyzed in each embryo. The average number of Pax6+ cells was obtained from three wild-type (two males and one female) and three premutation (three males) littermates. The average number of Tbr2+ cells was obtained from five wild-type (two females and three males) and five premutation (five males) age-matched mice, eight of which were littermates. We tested for gender differences and found none (see proliferation analysis below).

Proliferation analysis

Premutation versus wild-type. To determine whether the level of proliferation differed in wild-type versus premutation embryos, the number of mitoses was quantified based on

DAPI and 4A4 immunostaining. For DAPI analysis, the morphology of condensed chromatin (as characteristic of M-phase) was used to identify mitoses in DAPI-stained sections of wild-type and premutation mice. Equivalent sections from wild-type and premutation neocortex were incubated in DAPI (1:1000) for 10 min, sections were imaged on a confocal microscope and 200 μm wide bins were created that stretched from the ventricular surface to the pia in one optical plane of section. Mitoses were categorized based on location (at ventricular surface or at least one cell body away from ventricular surface). In addition, we compared the number of 4A4+ cells, which labels mitotic neural precursor cells (41), in wild-type and premutation embryos in 200 μm wide bins of neocortex. Three sequential coronal sections were quantified for each embryo to generate an average number and embryos were statistically compared across groups.

Male wild-type versus female wild-type. To determine whether the level of proliferation differed between genders, the number of mitoses was quantified in DAPI-stained sections of male and female wild-type mice. Equivalent sections of the neocortex from males and females were incubated in DAPI (1:1000) for 10 min, sections were imaged on a confocal microscope and 200 μm wide bins were created that stretched from the ventricular surface to the pia in one optical plane of section. Mitoses were categorized based on location (ventricular surface or at least one cell body away from ventricular surface). Three sequential coronal sections were quantified for each embryo to generate an average number and embryos were statistically compared across groups.

TUNEL assay

To determine whether the numbers of cells undergoing apoptosis or necrosis differed in the premutation and wild-type animals, a TUNEL assay was performed according to the manufacturer's instructions (Roche). Briefly, litter-matched controls and premutation embryos were removed, genotyped, fixed and cryostat sectioned as above. Sections were washed in 0.1 M PBS for 30 min and permeabilized in 0.1% Triton X-100 in 0.1% sodium citrate for 2 min on ice. Sections were then incubated in TUNEL reaction containing terminal deoxynucleotidyl transferase (TdT) and fluorescein-conjugated nucleotides for 1 h at 37°C. For negative controls, the TdT enzyme was omitted. For positive controls, the slices were incubated with 10 U/ml DNAse I (Roche) in 50 mM Tris–HCl, pH 7.5, 1 mg/ml BSA for 10 min at RT prior to treatment with the TUNEL reaction to induce free 3′-OHs on DNA characteristic of apoptosis. Slides were washed, cover slipped and imaged with a confocal microscope as described above.

Analysis of FMRP expression levels by western blotting

E15 embryos were removed from the uterus and tails clipped for genotyping to determine CGG repeat numbers (see *Genotyping* above). Brains were removed, the telencephalon isolated and frozen on dry ice. When CGG repeat numbers were obtained, telencephalons were homogenized with a dounce homogenizer in RIPA buffer containing protease inhibitors complete tablet (Roche). After homogenization, protein concentrations were determined using a BCA protein assay (Pierce). Fifty micrograms of protein were boiled for 5 min in 2X sample buffer and loaded onto a 4–20% SDS–PAGE gradient gel (Lonza). Three wild-type (10 CGG), three 100 CGG and three 150 CGG samples were loaded into individual lanes on the gel. The gel was run at 10 mA for 2 h to resolve individual proteins. The proteins were transferred onto a PVDF membrane (Millipore). The membrane was stained with Ponceau S (Sigma-Aldrich) to determine electrophoresis and transfer efficiency. The membrane was blocked by incubating in 5% non-fat milk solution for 2 h at RT. The membrane was incubated in chicken anti-FMRP (1:20 000) and mouse anti-beta-actin (1:4000, Abcam) in 5% non-fat milk solution, overnight at 4°C. Three washes of 15 min each followed by two washes of 5 min each were performed using wash buffer (0.1% Tween 20 in PBS). The membrane was then incubated in secondary antibody solution (donkey anti-chicken IR 800, 1:10 000, Licor; and goat anti-Mouse 680, 1:10 000, LiCor) in 5% non-fat milk solution, for 1 h at RT. The membrane was washed (three washes for 15 min each, followed by two washes for 5 min each) in wash buffer. The blot was then scanned using Odyssey Infrared Imager (Licor Biosciences, Lincoln, NE, USA). Densitometric analysis of western blot bands was performed using Image J. Statistical analysis was performed using Instat.

Statistical analysis

The genotype of tissue obtained from embryos was blinded before the orientation of eGFP-labeled migrating cells, the number of mitotic cells (4A4+ or DAPI), the number of Pax6+ or Tbr2+ cells or the number of TUNEL+ cells were quantified. *t*-Tests were performed to statistically compare the number of Pax6+ cells, Tbr2+ cells, mitotic DAPI or 4A4+ cells and the number of TUNEL+ cells between the premutation and wild-type littermate groups using GraphPad Instat (GraphPad Software, Inc.). The number of migrating cells that were classified as ventricular-directed, pial-directed or multipolar was statistically compared between the premutation and wild-type littermate groups with a Chi-square test (GraphPad Instat). The number of eGFP+ cells that were located in the VZ, SVZ, IZ or CP was statistically compared between groups with a Chi-square test (GraphPad Instat).

SUPPLEMENTARY MATERIAL

Supplementary Material is available at *HMG* online.

ACKNOWLEDGEMENTS

We thank Drs Fred Gage and Theo Palmer for providing the stably transfected retroviral packaging cell line; Lee Rognlie for assistance with animal mating and surgeries; Binh Ta and Glenda Espinal Goyne for genotyping and gender determination in the premutation and control embryos; Patricio Bravo Fuentes, Roxanne Parker, Katherine Hanel, Joseph Hamera and Matt Cziep for preparation and imaging of embryonic

neocortical tissue and Christine Iwahashi and Ryan Hunsaker for advice on the anti-chicken FMRP antibody.

Conflict of Interest statement. None declared.

FUNDING

This study was supported by NIH grants UL1 DEO19583, RL1 AG032119, and RL1 NS062411, the UC Davis M.I.N.D. Institute and the Children's Miracle Network.

REFERENCES

1. Amiri, K., Hagerman, R.J. and Hagerman, P.J. (2008) Fragile X-associated tremor/ataxia syndrome: an aging face of the fragile X gene. *Arch. Neurol.*, **65**, 19–25.
2. Berry-Kravis, E., Abrams, L., Coffey, S.M., Hall, D.A., Greco, C., Gane, L.W., Grigsby, J., Bourgeois, J.A., Finucane, B., Jacquemont, S. *et al.* (2007) Fragile X-associated tremor/ataxia syndrome: clinical features, genetics, and testing guidelines. *Mov. Disord.*, **22**, 2018–2030, quiz 2140.
3. Bourgeois, J.A., Coffey, S.M., Rivera, S.M., Hessl, D., Gane, L.W., Tassone, F., Greco, C., Finucane, B., Nelson, L., Berry-Kravis, E. *et al.* (2009) A review of fragile X premutation disorders: expanding the psychiatric perspective. *J. Clin. Psychiatry*, **70**, 852–862.
4. Brouwer, J.R., Willemsen, R. and Oostra, B.A. (2009) The FMR1 gene and fragile X-associated tremor/ataxia syndrome. *Am. J. Med. Genet. B Neuropsychiatr. Genet.*, **150B**, 782–798.
5. Grigsby, J., Brega, A.G., Engle, K., Leehey, M.A., Hagerman, R.J., Tassone, F., Hessl, D., Hagerman, P.J., Cogswell, J.B., Bennett, R.E. *et al.* (2008) Cognitive profile of fragile X premutation carriers with and without fragile X-associated tremor/ataxia syndrome. *Neuropsychology*, **22**, 48–60.
6. Leehey, M.A., Berry-Kravis, E., Goetz, C.G., Zhang, L., Hall, D.A., Li, L., Rice, C.D., Lara, R., Cogswell, J., Reynolds, A. *et al.* (2008) FMR1 CGG repeat length predicts motor dysfunction in premutation carriers. *Neurology*, **70**, 1397–1402.
7. Seritan, A.L., Nguyen, D.V., Farias, S.T., Hinton, L., Grigsby, J., Bourgeois, J.A. and Hagerman, R.J. (2008) Dementia in fragile X-associated tremor/ataxia syndrome (FXTAS): comparison with Alzheimer's disease. *Am. J. Med. Genet. B Neuropsychiatr. Genet.*, **147B**, 1138–1144.
8. Chonchaiya, W., Schneider, A. and Hagerman, R.J. (2009) Fragile X: a family of disorders. *Adv. Pediatr.*, **56**, 165–186.
9. Bassell, G.J. and Warren, S.T. (2008) Fragile X syndrome: loss of local mRNA regulation alters synaptic development and function. *Neuron*, **60**, 201–214.
10. Hagerman, R.J., Rivera, S.M. and Hagerman, P.J. (2008) The fragile X family of disorders: a model for autism and targeted treatments. *Curr. Ped. Rev.*, **4**, 40–52.
11. Oostra, B.A. and Willemsen, R. (2009) FMR1: a gene with three faces. *Biochim. Biophys. Acta*, **1790**, 467–477.
12. Song, F.J., Barton, P., Sleightholme, V., Yao, G.L. and Fry-Smith, A. (2003) Screening for fragile X syndrome: a literature review and modelling study. *Health Technol. Assess.*, **7**, 1–106.
13. Hagerman, P.J. (2008) The fragile X prevalence paradox. *J. Med. Genet.*, **45**, 498–499.
14. Rodriguez-Revenga, L., Madrigal, I., Pagonabarraga, J., Xuncla, M., Badenas, C., Kulisevsky, J., Gomez, B. and Mila, M. (2009) Penetrance of FMR1 premutation associated pathologies in fragile X syndrome families. *Eur. J. Hum. Genet.*, **17**, 1359–1362.
15. Jacquemont, S., Hagerman, R.J., Leehey, M.A., Hall, D.A., Levine, R.A., Brunberg, J.A., Zhang, L., Jardini, T., Gane, L.W., Harris, S.W. *et al.* (2004) Penetrance of the fragile X-associated tremor/ataxia syndrome in a premutation carrier population. *JAMA*, **291**, 460–469.
16. Greco, C.M., Berman, R.F., Martin, R.M., Tassone, F., Schwartz, P.H., Chang, A., Trapp, B.D., Iwahashi, C., Brunberg, J., Grigsby, J. *et al.* (2006) Neuropathology of fragile X-associated tremor/ataxia syndrome (FXTAS). *Brain*, **129**, 243–255.
17. Tassone, F., Adams, J., Berry-Kravis, E.M., Cohen, S.S., Brusco, A., Leehey, M.A., Li, L., Hagerman, R.J. and Hagerman, P.J. (2007) CGG repeat length correlates with age of onset of motor signs of the fragile X-associated tremor/ataxia syndrome (FXTAS). *Am. J. Med. Genet. B Neuropsychiatr. Genet.*, **144B**, 566–569.
18. Leehey, M.A., Berry-Kravis, E., Min, S.J., Hall, D.A., Rice, C.D., Zhang, L., Grigsby, J., Greco, C.M., Reynolds, A., Lara, R. *et al.* (2007) Progression of tremor and ataxia in male carriers of the FMR1 premutation. *Mov. Disord.*, **22**, 203–206.
19. Soontarapornchai, K., Maselli, R., Fenton-Farrell, G., Tassone, F., Hagerman, P.J., Hessl, D. and Hagerman, R.J. (2008) Abnormal nerve conduction features in fragile X premutation carriers. *Arch. Neurol.*, **65**, 495–498.
20. Tassone, F., Hagerman, R.J., Taylor, A.K., Gane, L.W., Godfrey, T.E. and Hagerman, P.J. (2000) Elevated levels of FMR1 mRNA in carrier males: a new mechanism of involvement in the fragile-X syndrome. *Am. J. Hum. Genet.*, **66**, 6–15.
21. Kenneson, A., Zhang, F., Hagedorn, C.H. and Warren, S.T. (2001) Reduced FMRP and increased FMR1 transcription is proportionally associated with CGG repeat number in intermediate-length and premutation carriers. *Hum. Mol. Genet.*, **10**, 1449–1454.
22. Allen, E.G., He, W., Yadav-Shah, M. and Sherman, S.L. (2004) A study of the distributional characteristics of FMR1 transcript levels in 238 individuals. *Hum. Genet.*, **114**, 439–447.
23. Hagerman, P.J. and Hagerman, R.J. (2004) Fragile X-associated tremor/ataxia syndrome (FXTAS). *Ment. Retard. Dev. Disabil. Res. Rev.*, **10**, 25–30.
24. Greco, C.M., Hagerman, R.J., Tassone, F., Chudley, A.E., Del Bigio, M.R., Jacquemont, S., Leehey, M. and Hagerman, P.J. (2002) Neuronal intranuclear inclusions in a new cerebellar tremor/ataxia syndrome among fragile X carriers. *Brain*, **125**, 1760–1771.
25. Tassone, F., Iwahashi, C. and Hagerman, P.J. (2004) FMR1 RNA within the intranuclear inclusions of fragile X-associated tremor/ataxia syndrome (FXTAS). *RNA Biol.*, **1**, 103–105.
26. Arocena, D.G., Iwahashi, C.K., Won, N., Beilina, A., Ludwig, A.L., Tassone, F., Schwartz, P.H. and Hagerman, P.J. (2005) Induction of inclusion formation and disruption of lamin A/C structure by premutation CGG-repeat RNA in human cultured neural cells. *Hum. Mol. Genet.*, **14**, 3661–3671.
27. Hashem, V., Galloway, J.N., Mori, M., Willemsen, R., Oostra, B.A., Paylor, R. and Nelson, D.L. (2009) Ectopic expression of CGG containing mRNA is neurotoxic in mammals. *Hum. Mol. Genet.*, **18**, 2443–2451.
28. Willemsen, R., Hoogeveen-Westerveld, M., Reis, S., Holstege, J., Severijnen, L.A., Nieuwenhuizen, I.M., Schrier, M., van Unen, L., Tassone, F., Hoogeveen, A.T. *et al.* (2003) The FMR1 CGG repeat mouse displays ubiquitin-positive intranuclear neuronal inclusions; implications for the cerebellar tremor/ataxia syndrome. *Hum. Mol. Genet.*, **12**, 949–959.
29. Brouwer, J.R., Huizer, K., Severijnen, L.A., Hukema, R.K., Berman, R.F., Oostra, B.A. and Willemsen, R. (2008) CGG-repeat length and neuropathological and molecular correlates in a mouse model for fragile X-associated tremor/ataxia syndrome. *J. Neurochem.*, **107**, 1671–1682.
30. Hunsaker, M.R., Wenzel, H.J., Willemsen, R. and Berman, R.F. (2009) Progressive spatial processing deficits in a mouse model of the fragile X premutation. *Behav. Neurosci.*, **123**, 1315–1324.
31. Wenzel, H.J., Hunsaker, M.R., Greco, C.M., Willemsen, R. and Berman, R.F. (2010) Ubiquitin-positive intranuclear inclusions in neuronal and glial cells in a mouse model of the fragile X premutation. *Brain Res.*, **1318**, 155–166.
32. Chen, Y., Tassone, F., Berman, R.F., Hagerman, P.J., Hagerman, R.J., Willemsen, R. and Pessah, I.N. (2010) Murine hippocampal neurons expressing Fmr1 gene premutations show early developmental deficits and late degeneration. *Hum. Mol. Genet.*, **19**, 196–208.
33. Abitbol, M., Menini, C., Delezoide, A.L., Rhyner, T., Vekemans, M. and Mallet, J. (1993) Nucleus basalis magnocellularis and hippocampus are the major sites of FMR-1 expression in the human fetal brain. *Nat. Genet.*, **4**, 147–153.
34. Rife, M., Nadal, A., Mila, M. and Willemsen, R. (2004) Immunohistochemical FMRP studies in a full mutated female fetus. *Am. J. Med. Genet. A*, **124A**, 129–132.
35. de Diego Otero, Y.B., Bontekoe, C., Raghoe, P., Luteijn, T., Hoogeveen, A.T., Oostra, B.A. and Willemsen, R. (2000) Immunocytochemical and biochemical characterization of FMRP, FXR1P, and FXR2P in the mouse. *Exp. Cell Res.*, **258**, 162–170.

36. Hessl, D., Tassone, F., Loesch, D.Z., Berry-Kravis, E., Leehey, M.A., Gane, L.W., Barbato, I., Rice, C., Gould, E., Hall, D.A. *et al.* (2005) Abnormal elevation of FMR1 mRNA is associated with psychological symptoms in individuals with the fragile X premutation. *Am. J. Med. Genet. B Neuropsychiatr. Genet.*, **139B**, 115–121.
37. Goodlin-Jones, B.L., Tassone, F., Gane, L.W. and Hagerman, R.J. (2004) Autistic spectrum disorder and the fragile X premutation. *J. Dev. Behav. Pediatr.*, **25**, 392–398.
38. Iwahashi, C., Tassone, F., Hagerman, R.J., Yasui, D., Parrott, G., Nguyen, D., Mayeur, G. and Hagerman, P.J. (2009) A quantitative ELISA assay for the fragile x mental retardation 1 protein. *J. Mol. Diagn.*, **11**, 281–289.
39. Devys, D., Lutz, Y., Rouyer, N., Bellocq, J.P. and Mandel, J.L. (1993) The FMR-1 protein is cytoplasmic, most abundant in neurons and appears normal in carriers of a fragile X premutation. *Nat. Genet.*, **4**, 335–340.
40. Kamei, Y., Inagaki, N., Nishizawa, M., Tsutsumi, O., Taketani, Y. and Inagaki, M. (1998) Visualization of mitotic radial glial lineage cells in the developing rat brain by Cdc2 kinase-phosphorylated vimentin. *Glia*, **23**, 191–199.
41. Noctor, S.C., Flint, A.C., Weissman, T.A., Wong, W.S., Clinton, B.K. and Kriegstein, A.R. (2002) Dividing precursor cells of the embryonic cortical ventricular zone have morphological and molecular characteristics of radial glia. *J. Neurosci.*, **22**, 3161–3173.
42. Noctor, S.C., Martinez-Cerdeño, V. and Kriegstein, A.R. (2008) Distinct behaviors of neural stem and progenitor cells underlie cortical neurogenesis. *J. Comp. Neurol.*, **508**, 28–44.
43. Feng, Y., Gutekunst, C.A., Eberhart, D.E., Yi, H., Warren, S.T. and Hersch, S.M. (1997) Fragile X mental retardation protein: nucleocytoplasmic shuttling and association with somatodendritic ribosomes. *J. Neurosci.*, **17**, 1539–1547.
44. Weissman, T., Noctor, S.C., Clinton, B.K., Honig, L.S. and Kriegstein, A.R. (2003) Neurogenic radial glial cells in reptile, rodent and human: from mitosis to migration. *Cereb. Cortex*, **13**, 550–559.
45. Noctor, S.C., Flint, A.C., Weissman, T.A., Dammerman, R.S. and Kriegstein, A.R. (2001) Neurons derived from radial glial cells establish radial units in neocortex. *Nature*, **409**, 714–720.
46. Noctor, S.C., Martínez-Cerdeño, V., Ivic, L. and Kriegstein, A.R. (2004) Cortical neurons arise in symmetric and asymmetric division zones and migrate through specific phases. *Nat. Neurosci.*, **7**, 136–144.
47. van Praag, H., Schinder, A.F., Christie, B.R., Toni, N., Palmer, T.D. and Gage, F.H. (2002) Functional neurogenesis in the adult hippocampus. *Nature*, **415**, 1030–1034.
48. van Praag, H., Shubert, T., Zhao, C. and Gage, F.H. (2005) Exercise enhances learning and hippocampal neurogenesis in aged mice. *J. Neurosci.*, **25**, 8680–8685.
49. Kakita, A. and Goldman, J.E. (1999) Patterns and dynamics of SVZ cell migration in the postnatal forebrain: monitoring living progenitors in slice preparations. *Neuron*, **23**, 461–472.
50. Rakic, P. (1972) Mode of cell migration to the superficial layers of fetal monkey neocortex. *J. Comp. Neurol.*, **145**, 61–83.
51. Nadarajah, B., Alifragis, P., Wong, R.O. and Parnavelas, J.G. (2002) Ventricle-directed migration in the developing cerebral cortex. *Nat. Neurosci.*, **5**, 218–224.
52. Miyata, T., Kawaguchi, A., Okano, H. and Ogawa, M. (2001) Asymmetric inheritance of radial glial fibers by cortical neurons. *Neuron*, **31**, 727–741.
53. Rakic, P. (1988) Specification of cerebral cortical areas. *Science*, **241**, 170–176.
54. Altman, J. and Bayer, S.A. (1990) Prolonged sojourn of developing pyramidal cells in the intermediate zone of the hippocampus and their settling in the stratum pyramidale. *J. Comp. Neurol.*, **301**, 343–364.
55. Tabata, H. and Nakajima, K. (2003) Multipolar migration: the third mode of radial neuronal migration in the developing cerebral cortex. *J. Neurosci.*, **23**, 9996–10001.
56. Nadarajah, B., Alifragis, P., Wong, R.O.L. and Parnavelas, J.G. (2003) Neuronal migration in the developing cerebral cortex: observations based on real-time imaging. *Cereb. Cortex*, **13**, 607–611.
57. Parnavelas, J.G. (2002) The origin of cortical neurons. *Braz. J. Med. Biol. Res.*, **35**, 1423–1429.
58. Englund, C., Fink, A., Lau, C., Pham, D., Daza, R.A., Bulfone, A., Kowalczyk, T. and Hevner, R.F. (2005) Pax6, Tbr2, and Tbr1 are expressed sequentially by radial glia, intermediate progenitor cells, and postmitotic neurons in developing neocortex. *J. Neurosci.*, **25**, 247–251.
59. Noctor, S.C., Martínez-Cerdeño, V. and Kriegstein, A.R. (2007) Contribution of intermediate progenitor cells to cortical histogenesis. *Arch. Neurol.*, **64**, 639–642.
60. Raske, C. and Hagerman, P.J. (2009) Molecular pathogenesis of fragile X-associated tremor/ataxia syndrome. *J. Investig. Med.*, **57**, 825–829.
61. Primerano, B., Tassone, F., Hagerman, R.J., Hagerman, P., Amaldi, F. and Bagni, C. (2002) Reduced FMR1 mRNA translation efficiency in fragile X patients with premutations. *RNA*, **8**, 1482–1488.
62. Farzin, F., Perry, H., Hessl, D., Loesch, D., Cohen, J., Bacalman, S., Gane, L., Tassone, F., Hagerman, P. and Hagerman, R. (2006) Autism spectrum disorders and attention-deficit/hyperactivity disorder in boys with the fragile X premutation. *J. Dev. Behav. Pediatr.*, **27**, S137–S144.
63. Hagerman, R.J. (2006) Lessons from fragile X regarding neurobiology, autism, and neurodegeneration. *J. Dev. Behav. Pediatr.*, **27**, 63–74.
64. O'Rourke, N.A., Dailey, M.E., Smith, S.J. and McConnell, S.K. (1992) Diverse migratory pathways in the developing cerebral cortex. *Science*, **258**, 299–302.
65. Kriegstein, A.R. and Noctor, S.C. (2004) Patterns of neuronal migration in the embryonic cortex. *Trends Neurosci.*, **27**, 392–399.
66. Bayer, S.A. and Altman, J. (1991) *Neocortical Development*. Raven Press, New York.
67. Chen, G., Sima, J., Jin, M., Wang, K.Y., Xue, X.J., Zheng, W., Ding, Y.Q. and Yuan, X.B. (2008) Semaphorin-3A guides radial migration of cortical neurons during development. *Nat. Neurosci.*, **11**, 36–44.
68. Morita, A., Yamashita, N., Sasaki, Y., Uchida, Y., Nakajima, O., Nakamura, F., Yagi, T., Taniguchi, M., Usui, H., Katoh-Semba, R. *et al.* (2006) Regulation of dendritic branching and spine maturation by semaphorin3A-Fyn signaling. *J. Neurosci.*, **26**, 2971–2980.
69. Jan, Y.N. and Jan, L.Y. (2010) Branching out: mechanisms of dendritic arborization. *Nat. Rev. Neurosci.*, **11**, 316–328.
70. Sang, Q. and Tan, S.S. (2003) Contact-associated neurite outgrowth and branching of immature cortical interneurons. *Cereb. Cortex.*, **13**, 677–683.
71. Wegiel, J., Kuchna, I., Nowicki, K., Imaki, H., Marchi, E., Ma, S.Y., Chauhan, A., Chauhan, V., Bobrowicz, T.W., de Leon, M. *et al.* (2010) The neuropathology of autism: defects of neurogenesis and neuronal migration, and dysplastic changes. *Acta Neuropathol*, **119**, 755–770.
72. Moro, F., Pisano, T., Bernardina, B.D., Polli, R., Murgia, A., Zoccante, L., Darra, F., Battaglia, A., Pramparo, T., Zuffardi, O. *et al.* (2006) Periventricular heterotopia in fragile X syndrome. *Neurology*, **67**, 713–715.
73. Sessa, A., Mao, C.A., Hadjantonakis, A.K., Klein, W.H. and Broccoli, V. (2008) Tbr2 directs conversion of radial glia into basal precursors and guides neuronal amplification by indirect neurogenesis in the developing neocortex. *Neuron*, **60**, 56–69.
74. Tervonen, T.A., Louhivuori, V., Sun, X., Hokkanen, M.E., Kratochwil, C.F., Zebryk, P., Castren, E. and Castren, M.L. (2009) Aberrant differentiation of glutamatergic cells in neocortex of mouse model for fragile X syndrome. *Neurobiol. Dis.*, **33**, 250–259.
75. Sessa, A., Mao, C.A., Colasante, G., Nini, A., Klein, W.H. and Broccoli, V. (2010) Tbr2-positive intermediate (basal) neuronal progenitors safeguard cerebral cortex expansion by controlling amplification of pallial glutamatergic neurons and attraction of subpallial GABAergic interneurons. *Genes Dev.*, **24**, 1816–1826.
76. Arnold, S.J., Hofmann, U.K., Bikoff, E.K. and Robertson, E.J. (2008) Pivotal roles for eomesodermin during axis formation, epithelium-to-mesenchyme transition and endoderm specification in the mouse. *Development*, **135**, 501–511.
77. Tassone, F., Beilina, A., Carosi, C., Albertosi, S., Bagni, C., Li, L., Glover, K., Bentley, D. and Hagerman, P.J. (2007) Elevated FMR1 mRNA in premutation carriers is due to increased transcription. *RNA*, **13**, 555–562.
78. Brouwer, J.R., Mientjes, E.J., Bakker, C.E., Nieuwenhuizen, I.M., Severijnen, L.A., Van der Linde, H.C., Nelson, D.L., Oostra, B.A. and Willemsen, R. (2007) Elevated Fmr1 mRNA levels and reduced protein expression in a mouse model with an unmethylated Fragile X full mutation. *Exp. Cell Res.*, **313**, 244–253.
79. Jin, P., Zarnescu, D.C., Zhang, F., Pearson, C.E., Lucchesi, J.C., Moses, K. and Warren, S.T. (2003) RNA-mediated neurodegeneration caused by the fragile X premutation rCGG repeats in Drosophila. *Neuron*, **39**, 739–747.
80. Hagerman, P.J. and Hagerman, R.J. (2004) The fragile-X premutation: a maturing perspective. *Am. J. Hum. Genet.*, **74**, 805–816.

81. Sellier, C., Rau, F., Liu, Y., Tassone, F., Hukema, R.K., Gattoni, R., Schneider, A., Richard, S., Willemsen, R., Elliott, D.J. *et al.* (2010) Sam68 sequestration and partial loss of function are associated with splicing alterations in FXTAS patients. *EMBO J.*, **29**, 1248–1261.
82. Huot, M.E., Vogel, G. and Richard, S. (2009) Identification of a Sam68 ribonucleoprotein complex regulated by epidermal growth factor. *J. Biol. Chem.*, **284**, 31903–31913.
83. Mulders, S.A., van Engelen, B.G., Wieringa, B. and Wansink, D.G. (2010) Molecular therapy in myotonic dystrophy: focus on RNA gain-of-function. *Hum. Mol. Genet.*, **19**, R90–R97.
84. Brown, V., Jin, P., Ceman, S., Darnell, J.C., O'Donnell, W.T., Tenenbaum, S.A., Jin, X., Feng, Y., Wilkinson, K.D., Keene, J.D. *et al.* (2001) Microarray identification of FMRP-associated brain mRNAs and altered mRNA translational profiles in fragile X syndrome. *Cell*, **107**, 477–487.
85. Penagarikano, O., Mulle, J.G. and Warren, S.T. (2007) The pathophysiology of fragile x syndrome. *Annu. Rev. Genomics Hum. Genet.*, **8**, 109–129.
86. Darnell, J.C., Jensen, K.B., Jin, P., Brown, V., Warren, S.T. and Darnell, R.B. (2001) Fragile X mental retardation protein targets G quartet mRNAs important for neuronal function. *Cell*, **107**, 489–499.
87. Dickson, B.J. (2002) Molecular mechanisms of axon guidance. *Science*, **298**, 1959–1964.
88. Ito, K., Kawasaki, T., Takashima, S., Matsuda, I., Aiba, A. and Hirata, T. (2008) Semaphorin 3F confines ventral tangential migration of lateral olfactory tract neurons onto the telencephalon surface. *J. Neurosci.*, **28**, 4414–4422.
89. Luo, Y., Shan, G., Guo, W., Smrt, R.D., Johnson, E.B., Li, X., Pfeiffer, R.L., Szulwach, K.E., Duan, R., Barkho, B.Z. *et al.* (2010) Fragile x mental retardation protein regulates proliferation and differentiation of adult neural stem/progenitor cells. *PLoS Genet.*, **6**, e1000898.
90. Callan, M.A., Cabernard, C., Heck, J., Luois, S., Doe, C.Q. and Zarnescu, D.C. (2010) Fragile X protein controls neural stem cell proliferation in the Drosophila brain. *Hum. Mol. Genet.*, **19**, 3068–3079.
91. Tassone, F., Pan, R., Amiri, K., Taylor, A.K. and Hagerman, P.J. (2008) A rapid polymerase chain reaction-based screening method for identification of all expanded alleles of the Fragile X (FMR1) gene in newborn and high-risk populations. *J. Mol. Diagn.*, **10**, 43–49.
92. Bontekoe, C.J., de Graaff, E., Nieuwenhuizen, I.M., Willemsen, R. and Oostra, B.A. (1997) FMR1 premutation allele (CGG)81 is stable in mice. *Eur. J. Hum. Genet.*, **5**, 293–298.
93. Palmer, T.D., Markakis, E.A., Willhoite, A.R., Safar, F. and Gage, F.H. (1999) Fibroblast growth factor-2 activates a latent neurogenic program in neural stem cells from diverse regions of the adult CNS. *J. Neurosci.*, **19**, 8487–8497.
94. Burns, J.C., Friedmann, T., Driever, W., Burrascano, M. and Yee, J.K. (1993) Vesicular stomatitis virus G glycoprotein pseudotyped retroviral vectors: concentration to very high titer and efficient gene transfer into mammalian and nonmammalian cells. *Proc. Natl Acad. Sci.*, **90**, 8033–8037.